Plasmonic enhancement of single-molecule fluorescence under one- and two-photon excitation

Lu, X.

1

Introduction

1

Collecting photons by eyes is probably one of the most efficient ways for us to perceive the environment. For centuries, great efforts have been made to extend our visual range by manipulating the propagation of light, e.g. through a telescope or microscope, we can see further or smaller into the world. Visualizing optically at micron or submicron length scales helps to reveal many secrets hidden to our naked eyes, especially in the biological systems. Recent technical advances in optics have pushed the detection capability down to the single-molecule level, giving a new access to the unique properties of individual molecules that usually cannot be distinguished in ensemble experiments[1, 2]. Single-molecule techniques have soon grown into an important field of optics, and spawned a revolution in biophysics/chemistry and other fields of nanoscience[3–10].

The challenge of detecting a single molecule optically comes from the mismatch between the molecular sizes and the wavelength of light, which results in very weak interactions between individual molecules and light[11, 12]. Pioneered by Orrit and Bernard in 1990[13], fluorescence, with the photons emitted at a longer wavelength than the excitation light (Stokes-shifted)[14], has been recognized as one of the most convenient means of probing single molecules, as the background can be suppressed efficiently by spectral filtering[15–18]. The fluorescence-based single-molecule technique, however, relies on the contrast provided by the emission of the target molecules against the background scattering and the photons from the environmental molecules. Therefore, this technique can only be applied to strong emitters (e.g. with quantum yields $> 10\%$), which limits its applications since the majority of molecules only emit weakly. Additionally, low molecular concentration ($\mathrm{pM} \sim \mathrm{nM}$) is required to get single-molecule sensitivity in conventional microscopy due to the diffraction limit of excitation beams[19].

Plasmonics nanostructures, well known for their subwavelength light confinements, offer a versatile solution to improve the detection sensitivity of single weak emitters by enhancing their fluorescence. The enhanced fluorescence from the molecules of low quantum yield ($10^{-1} \sim 10^{-3}$) inside the nanoscale near-field region, can easily overcome the total emission background from all the non-enhanced molecules in the micron-scale focusing volume, even for concentrations as high as μM[20]. Despite many successes of plasmon enhanced fluorescence experiments, detecting ultra-weak photon emission at single-molecule level is still a challenge. Example comes from the molecules with extremely low quantum yields (e.g. $< 10^{-3}$)[21], or with very low excitation efficiency, such as the fluorescence under two-photon excitation[22, 23].

This thesis aims to improve the detection from ultra-weak single emitter by enhancing their emission properties with plasmonic nanostructures. We exploit the wet-chemically synthesized single crystalline gold nanorods (GNRs) as our basic frameworks in the whole studies, simply because of their unique optical properties, such as the intense electromagnetic fields enhancement near the tips, and the narrow, tunable resonance with light. We first explore the lower limit of fluorescence quantum yield for single-molecule detection by enhancing the fluorescence with a single gold nanorod. Later, we develop a method to synthesize end-to-end gold nanorod dimers on glass substrates with the aid of molecular linkers, and then apply these strong plasmon coupling systems to enhance the single-molecule fluorescence under two-photon excitation.

1.1. Surface plasmon resonance of gold nanoparticles

Propagating and localized surface plasmons

"Surface plasmons" (SPs) refers to the collective oscillations of conduction electrons that exists at the metal-dielectric interfaces. While still a hot topic of research, the observations and applications of SPs has a long history and can be dated back to Roman empire. The famous example is the Lycurgus cup, which shows different color depending on the location of the light source. A theoretical description of SPs however came only after Gustav Mie gave the first full solution to the scattering of light by a spherical metallic particle in 1908[24], and was explained as the coherent oscillation of electrons at metal surfaces by Rufus Ritchie in 1957[25].

Surface plasmons can be categorized into two main subclasses: the propagating SP polaritons (SPPs) waves that travel along the metal-dielectric interface at a wavelength shorter than the free light in the dielectric material[25–29], and the localized SPs (LSPs) modes that are excited in the metal structures with sizes comparable to or smaller than the exciting light, such as metal nanoparticles[30–32]. Although both the SPPs and LSPs can remarkably enhance the electromagnetic fields near the surfaces, the LSPs are more favored for singe-molecule sensing, primarily because the LSPs are more convenient to excite (no requirement on the momentum of the exciting light), and the near fields of LSPs are more localized into a small volume, instead of distributed widely around the interfaces as the propagating modes. Additionally, they also benefit from the cheap but reliable synthesis of metallic nanoparticles, with their shapes and sizes being adjustable to tune their plasmon resonances[33].

Localized surface plasmons of gold nanoparticles

Among different types of plasmoics nanoparticles, wet-chemcally systhesized gold nanoparticles have attracted most attention, mainly because of their chemical stability and the excellent performance in the visible and NIR spectral ranges. As a straightforward example, a single gold nano-sphere shows a strong plasmon resonance in the visible range around $520 \sim 580\ \mathrm{nm}$, when its size is smaller than $100\ \mathrm{nm}$ (see figure 1.1a)[34]. The strong scattering and absorption of light in this color range by the gold nanoparticles can explain the secret of the orientation-dependent color change of the Lycurgus cup, which contains tiny gold nanoparticles dispersing in the glass. The gold nanoparticle also exhibits nanofocusing ability of electromagnetic fields. As is depicted in figures 1.1c. and 1.1e., the electric field is localized at the surface of the gold nanosphere at resonance, and the intensity reduces rapidly in a few nanometers away from the surface, depending on the size of the particles.

The limitation of spherical gold nanoparticles for single-molecule sensing arises from their small field enhancements. As is shown in Figure 1c., the maximum field enhancement given by a gold nanosphere only reaches the magnitude of 10^1, which is usually too low for enhancing weak signals from single molecules. Additionally, the tunable spectral range, corresponding to enhancement by the narrow dipole plasmonic mode, covers only small range of visible light (e.g. $520 \sim 580\ \mathrm{nm}$ for particle size $\leq 100\ \mathrm{nm}$), which further limits their applications to a few favourable emitters. Extending to longer wavelength can

1

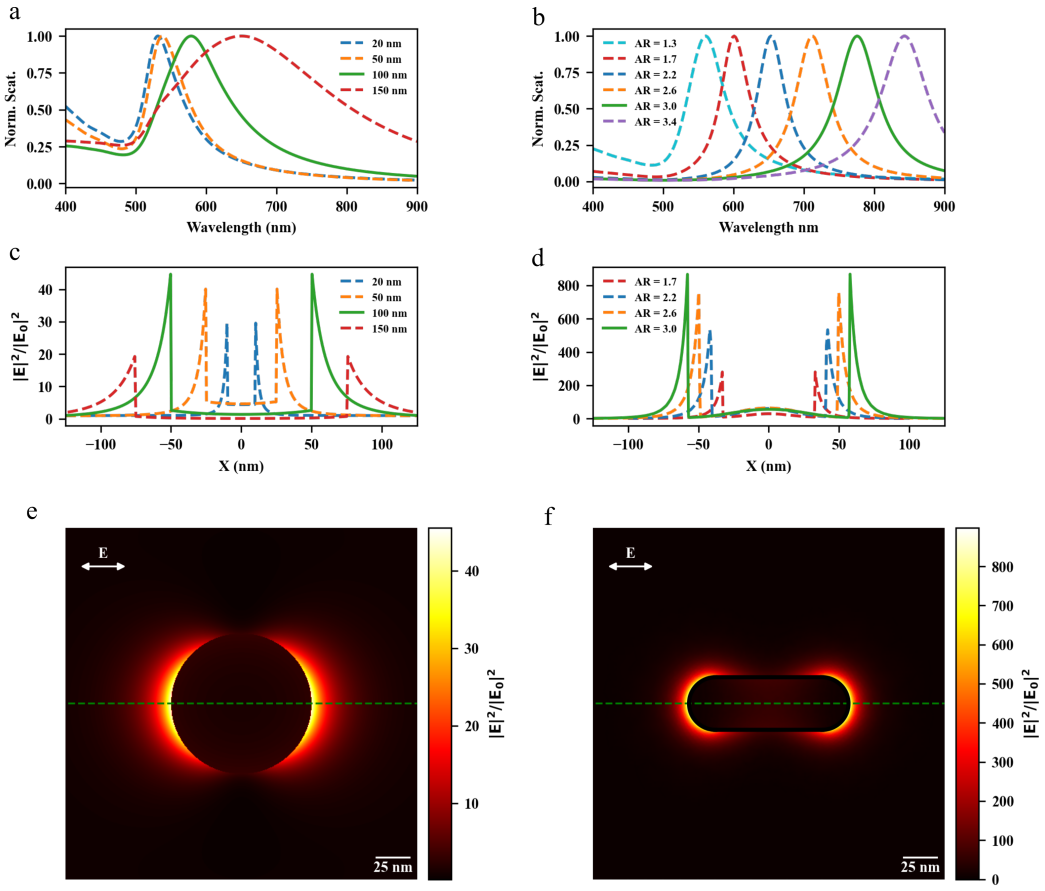

Figure 1.1: Surface plasmons of single gold nanospheres and gold nanorods in water. (a, b) Simulated scattering spectra of the gold nanospheres (a) and nanorods (b) excited by a linear polarized plane wave. In the simulations, Mie theory was performed for the spherical particles of varied sizes (here, 20, 50, 100, and 150 nm), and the boundary element method was used for the nanorods with a fixed diameter of 38 nm but with different aspect ratios. (c, d) The corresponding electric field intensity distributions along the main axis (green dashed in e and f) of the gold nanoparticles (c) and nanorods (d) at resonance. (e, f) The electric field intensity profile around the resonant gold nanosphere (e) and gold nanorod (f), corresponding to the size of 100 nm for the nanosphere, and 38 nm $\times$ 114nm for the nanorod.

be done by choosing a larger nanoparticle , yet, increasing the size (e.g. $> 150\ \mathrm{nm}$) results in a smaller near-field enhancement (red dashed in figure 1.1.c.) and larger luminescence background from the particles as the result of the broad plasmon resonance (red dashed in figure 1.1a.).

Localized surface plasmons of gold nanorods

Compared to gold nanospheres, the elongated gold nanorods (GNRs) exhibit better optical performance in nanofocusing[35]. As an anisotropic structure, GNRs support two primary plasmonic modes, the transverse mode and the longitudinal mode, corresponding to electron oscillations perpendicular or parallel to the longitudinal axis, respectively[36]. While the transverse modes display constant resonance at around $514\ \mathrm{nm}$, the longitudinal modes are more sensitive to the particle shapes, and can be well tuned from visible to near infrared region by adjusting their aspect ratio. As the resonances are further away from the interband transition band of gold, the damping effect due to Ohmic loss becomes weaker, resulting in narrower resonance bands as is shown in figure 1.1b.. The intense plasmon gives rise to very large near-field enhancement near the tips (see figures 1.1d., and 1.1e.), a feature that have been widely used to enhance weak signals, such as Raman scattering or fluorescence from single molecules. The longitudinal plasmon modes of GNRs are also very sensitive to the surrounding environment[37, 38]. As an example, by monitoring the plasmon shifts of GNRs, one might even be able to sense the tiny refractive index changes caused by the approach of a small object, such as a single protein molecule[39].

The applications of GNRs are also inspired by their chemical stability and by the flexibility of tuning their sizes and shapes. The sizes and aspect ratios of GNRs can be readily controlled during the synthesis process[40, 41], or can be adjusted by overgrowth or oxidation of the GNRs[42]. As a result, the plasmon resonances of GNRs can be tuned to cover a broader range of molecular absorbance bands, hence extends their applications to more species of molecules. GNRs are also suitable for biological applications because of their biocompatibility[43]. They can be conveniently functionalized with different molecules, including drug- or bio-molecules, though the high affinity of gold towards thiols[44, 45]. Moreover, the molecules can be specifically functionalized to the tips or to side of GNRs, as a result of the site-dependent reactivity of GNRs. The site-specifically functionalization of GNRs offers more controllable ways to study the interaction of molecules with the longitudinal plasmon modes. For example, the tip-specific functionalization of GNRs can improve the detection sensitivity of single molecules as the molecules can specifically be located inside the nearfield hotspots to get maximum signals enhancements[46, 47].

Plamonic coupling of end-to-end gold nanorod dimers

The plasmon resonance of a plasmonic nanostructure can be significantly modified by coupling with other nanostructures. Inspired by molecular orbital theory, the plasmon resonances resulting from plasmonic coupling can be regarded as the hybridization of the basic plasmon resonances of each component[48–50]. The hybridized plasmon resonances can be classified according to the relative oscillating behaviors of all the basic plasmon modes, or simply categorized into dark modes and bright modes according to their response to the

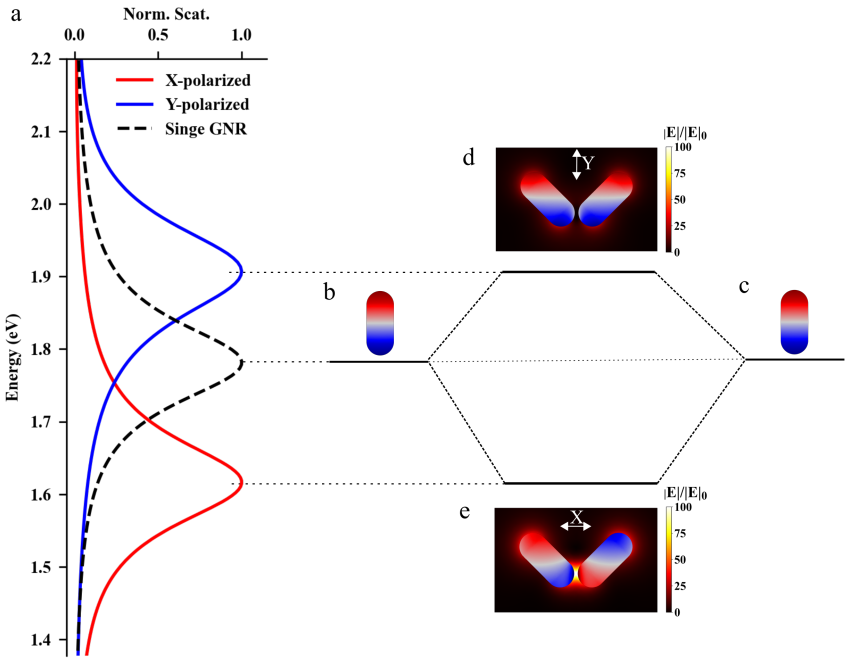

Figure 1.2: Plasmonic hybridization of a v-shaped gold nanorod dimer in the medium water ($n = 1.33$). (a) The black dashed line represents the scattering spectrum of the single GNR with the size of $40\ \mathrm{nm} \times 94\ \mathrm{nm}$, while the blue and red solid lines give the scattering spectra for the v-shaped GNRs dimer excited by light with the polarization perpendicular (S-polarized) and parallel (P-polarized) to the symmetry axis, respectively. The structure of the dimer was set as $\pi/2$ and the interparticle gap was set as $5\ \mathrm{nm}$. (b, c) The surface charge profile of the single GNR at the plasmonic resonance, (d, e) give the surface charges and the near-field profiles of the two hybridized plasmonic modes oscillating symmetrically and anti-symmetrically, respectively. In the simulations, the scattering spectra were calculated by using the boundary element method (Scuff-Em), while the near-fields and the surface charges were simulated with COMSOL Multiphysics.

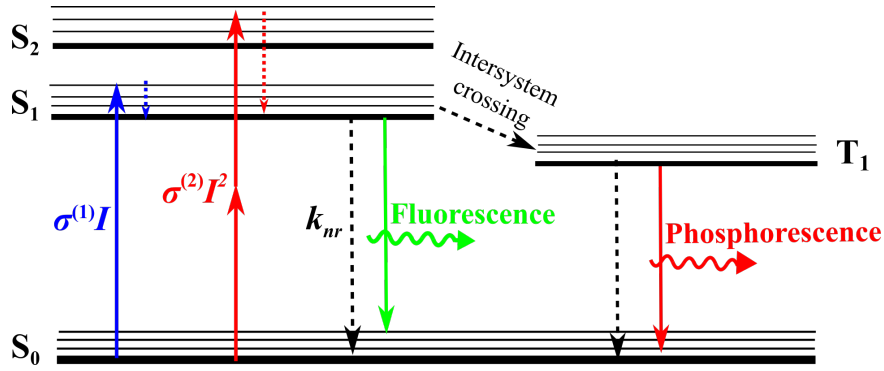

Figure 1.3: Jablonski diagram illustrating the light emission process under one-photon or two-photon excitation. $\sigma^{(1)}$ and $\sigma^{(2)}$ represent the one- and two-photon absorption cross-sections, respectively, I is the intensity of excitation photon flux, and k_{nr} is the non-radiative rate.

excitation light. The dark plasmon modes are usually hard to excite with plane light waves, while the bright modes show strong reaction to the incident light, resulting in large interaction cross sections and strong near field enhancements in some of the interparticle gaps[51].

The plasmonic coupling of nanostructures is determined by the materials, shapes, sizes, and the arrangements of all the coupling components. As a simple example depicted in figure 3., the plasmon resonance of a symmetric v-shaped GNRs dimer nanostructure splits into a symmetric (bonding) low-energy mode, and a anti-symmetric (anti-bonding) high-energy mode. The bonding or anti-bonding modes of the GNRs dimer can be excited by normal incident plane light with polarization perpendicular or parallel to the symmetry axis, respectively. Similar to the electron distribution of a covalent bonding molecule, the electromagnetic field profiles of the v-shaped GNRs dimer are also dependent on the symmetry of the plasmon oscillations. For the bonding mode, the near-field is strongly confined in the small gaps of the dimer, while for the anti-bonding mode, the field is localized with smaller enhancement around the far ends of the GNRs . The plasmon resonances of these two modes are also dependent on the angle between the long axes of the two GNRs. As the long axes of two GNRs are aligned along each other, only the bonding mode can be excited, and the anti-bonding mode at the shorter wavelength is hidden in the spectra, corresponding respectively to the bright and dark modes mentioned above[52, 53].

1.2. Fluorescence and fluorescence enhancement

One-photon-excited fluorescence

Materials can emit photons as they are excited to high energy levels. If the excitation is due to the absorption of photons, the emission is called photoluminescence. Fluorescence refers to the photoluminescence while the photon is emitted subsequently (in the timescale of sub-nanosecond or nanosecond) after the absorption of one photon[14]. For normal molecules at room temperature, the emission photons usually have longer wavelength compared to the excitation, a phenomenon called Stokes shift. The energy loss of the emitted photon is due

to the nonradiative relaxation of the excited molecule from the higher vibrational sub-levels to the lowest level of the excited electron state, as is depicted in figure 1.3. After a time of sub-nanosecond to ~ 10 ns, the molecule is then dissipated to the ground state by emitting a photon, or though other nonradiative pathways. Alternatively, the molecule may also be transferred to the lowest excited triplet state (T_1), a dark state where the molecule can stay for a time scale of microseconds before nonradiatively relaxing to the ground state. The random switching between the bright state (S_1) and the dark state (T_1) results in a phenomenon known as fluorescence blinking, where the molecule enters nonfluorescent state repeatedly under continuous excitation. Here we should mention that, at low temperature, the molecule at the triplet state (T_1) can also emit photon, a process called phosphorescence.

The excitation rate of one-photon excitation (OPE) $k_{\mathrm{exc}}^{(1)}$ below saturation is proportional to the photon flux intensity of the excitation I_{exc} as: $k_{\mathrm{exc}}^{(1)} = \sigma^{(1)} I_{\mathrm{exc}}$, where $\sigma^{(1)}$ is the one-photon absorption cross section of the molecule. Considering the long lifetime of the triplet state, the contribution of the intersystem crossing rate (k_{iSC}) to the total relaxing rate is often negligible, therefore the quantum yield of a fluorophore can be simply expressed as

$$\eta = k_{\mathrm{r}}/(k_{\mathrm{r}} + k_{\mathrm{nr}}) \tag{1.1}$$

here, k_{r} is the radiative rate, which is determined by the local density of photon states, and k_{nr} is the nonradiative rate. For a great majority of strongly absorbing molecules, the nonradiative rate dominates the deactivation process of the excited state to the ground state ($k_{\mathrm{nr}} \gg k_{\mathrm{r}}$), hence inhibits the spontaneous emissions of the molecules, resulting in very weak emitters that are very difficult to detect.

Two-photon-excited fluorescence

Instead of being excited by only one photon, the fluorophores can also be excited by multiple photons of lower energy. The simplest variant of multi-photon excitation is two-photon excitation, where the molecule is excited by absorbing two photons of identical frequencies simultaneously. Two-photon excitation (TPE) is a nonlinear optical process where the excitation rate $k_{\mathrm{exc}}^{(2)}$ is proportional to the square of the incident light intensity $k_{\mathrm{exc}}^{(2)} = \sigma^{(2)} I_{\mathrm{exc}}^2$[54], where $\sigma^{(2)}$ is the two-photon absorption cross section. TPE extends the absorption band into longer wavelength, usually in the infrared range, by exciting with two photons of the same wavelength. The excitation wavelength of TPE, however, is not necessary the double of OPE, as the molecules under TPE may be excited to different excited electron state due to the different selection rule for TPE. The emission spectra, however, is identical to one-photon-excited fluorescence, as the molecule only emits from the lowest level of the excited state S_1, according to the Kasha's rule. As a result, the lifetime and the quantum yield of the molecules under two-photon-excitation will be similar as those of one-photon-excited fluorescence.

TPE spectroscopy has attracted significant research interests because of its advantages over its OPE counterpart: 1), TPE facilities tissue penetration and background suppression as the result of the longer excitation wavelength, which may fall into the "biological transparency window"[55, 56]; 2), TPE allows inherent optical sectioning without the need of rejecting the out-of-focus emission, as the excitation under TPE is limited to a small volume, due to squared dependence of TPE on the incident light[57–59]; 3), for the same reason,

TPE also avoids out-of-focus photobleaching, which allows multiple scanning with reduced photodamage to the samples[60, 61].

The major obstruction for the application of TPE comes from the extremely low TPE efficiency which requires very high excitation intensity. Since first predicted by Goppert Mayer in 1931[54], TPE was only experimentally verified until the invention of lasers in 1960s, which could provide enough coherent photons for TPE[62, 63]. Yet illumination by light with very high power may also cause unacceptable photodamge to the samples. Ultra-short-pulsed laser, being able to generate ultra-high pulse intensities while still keeping the average output power relatively low, have stimulated the rapid growth of TPE's applications since its invention in 1990s[57]. Investigation of TPE at single-molecule level, however, is still a challenge. The TPA cross section for normal dyes is very low due to their small sizes ($1 \sim 3$ nm), typically in the range of $10^0 \sim 10^2$ GM (Goppert-Mayer), while $1\ \mathrm{GM} = 10^{-50}\mathrm{cm}^4\mathrm{s}\ \mathrm{molecule}^{-1}\ \mathrm{photon}^{-1}$[64–66].

Plasmonic enhancement of single-molecule fluorescence

The essential difficulty of detecting a single weak emitter is how to extract the weak signals from the background. In normal microscopy, limited by the diffraction of light, "selective" excitation of a particular molecule while keeping the surrounding molecules unexcited is very difficult, especially when the molecular concentration is high. By utilizing nano plasmonic lenses, one can create "superemitters" with enhanced fluorescence intensities overwhelm the brightness of the surrounding molecules. The enhancement of the fluorescence arises from the enhancement of the exciting electric field and from the enhancement of the radiative rate by coupling the emitters with the plasmonic nanoparticles. First of all, the excitation rate k_{exc} can be highly enhanced in the vicinity of the nanoparticle as a result of the strong electromagnetic field confinement. The enhancement factor ξ_{exc} shows different intensity dependence for OPE and for TPE on the excitation power: for OPE, ξ_{exc} is proportional to the enhancement of the near-field intensity, while for TPE, it scales with the square of the enhancement of the excitation light intensity. Secondly, the spontaneous emission k_{r} of the fluorophore can also be enhanced by the particle via the Purcell effect, which is related to the local density of photon states. Associated to the dissipative losses of the metals, however, coupling with the plasmon modes may also introduce additional non-radiative decay channels, which may quench the fluorescence of the molecules. The balance between the enhancement and the quenching strongly depends on the relative position and orientation of the emitter with respect to the nanoparticles, which may change the spectral shapes of the emissions and the lifetimes. The enhancement factor can be tuned by adjusting the sizes, shapes and the configurations of the nanoparticles.

Considering the simple two-level scheme, the overall enhancement under weak excitation can be expressed as[21, 67]

$$\xi_{\mathrm{total}} = \frac{\xi_{\mathrm{exc}}\xi_{\mathrm{rad}}}{1 + \eta_0(\xi_{\mathrm{rad}} + K_{\mathrm{nr}}/k_{\mathrm{r}}^0 - 1)}, \tag{1.2}$$

here, ξ_{exc} represents the excitation enhancement, $\xi_{\mathrm{rad}} = k_{\mathrm{r}}/k_{\mathrm{r}}^0$ is the radiative enhancement factor, which accounts for the increased local density of states in the vicinity of the antenna . k_r and k_r^0 are the radiative decay rates with and without the nanoantenna, respectively,

η_0 is the intrinsic quantum yield of the emitter, and K_{nr} is the additional non-radiative absorption rate due to dissipative losses of the nanoantenna. The lifetime of the fluorescence is shortened as[22]

$$\tau/\tau_0 = \eta_0^{-1}(\xi_{\mathrm{rad}} + K_{\mathrm{nr}}/k_{\mathrm{r}}^0 + 1/\eta_0 - 1)^{-1} \tag{1.3}$$

1.3. Outline of the thesis

This thesis examines the single-molecule detection of very weak optical signals enhanced by gold-nanorod-based plasmonic nanostructures. We first used single gold nanorods to enhance the conventional one-photon-excited fluorescence from single molecules with extremely low quantum yield ($\eta \sim 10^{-4}$). Later, we explored single-molecule detection of the fluorescence under two-photon-excitation enhanced by end-to-end gold nanorod dimer. Further experiments confirmed that such gold nanorod dimers may also be used to enhance the anti-Stokes Raman scattering, once the strong plasmon coupling between each rod not only strongly enhance the nearfield but also heat up the medium around the molecules inside the gap. The contents of the thesis is organized as follows:

In **Chapter 2**, we give general evaluation of single-molecule fluorescence with the enhancement by gold-nanorod-related plasmonic nanostructures. We performed full-wave simulations based on the boundary element method to estimate the fluorescence enhancement factor under OPE or TPE, by single gold nanorods, or by end-to-end gold nanorod dimers. The modification of the emission spectra and of the fluorescence lifetime by the plasmon modes are also investigated theoretically.

Chapter 3 demonstrates the single-molecule detection of a very weak emitter with a quantum yield of about 10^{-4} and a comparatively large Stokes shift of $3000\ \mathrm{cm}^{-1}$, by enhancing the fluorescence with single gold nanorods. We optimize the fluorescence rates by optimizing the excitation wavelength and the plasmon resonance. We further theoretically estimated that the quantum yield detection limit of a single molecule could be as low as 10^{-6}, provided the dwell time of the molecules in the plasmonic hot spot is long enough.

In **Chapter 4**, we develop a method to synthesize end-to-end gold nanorod dimers with the aid of molecular linkers. We controlled the end-to-end assembly in the presence of CTAB surfactant, which forms a bilayer that coats more compact over the side of the rods, to favor the attachment of the linker molecules at the tips. The interparticle gaps were kept open by choosing biomolecule pairs of streptavidin and biotin disulfide as the linkers, which ensures a separation of around $5\ \mathrm{nm}$ between the two nanorods.

In **Chapter 5**, we exploit the end-to-end gold nanorod dimer to enhance the two-photon-excited fluorescence of a single organic molecule. The strong plasmon coupling between the rods induces a very intense local field in the gap, with the maximum enhancement factor up 10^2, resulting in a TPE enhancement of $10^7 \sim 10^8$. With such high enhancement factor, we successfully detected two-photon-excited fluorescence at single-molecule level. Correlated scanning electron microscope images (SEM) were taken later to examine the configurations of the gold nanorod dimer structures.

References

[1] W. E. Moerner and Michel Orrit. Illuminating Single Molecules in Condensed Matter. *Science*, 283(5408):1670–1676, March 1999.

[2] David R. Walt. Optical Methods for Single Molecule Detection and Analysis. *Analytical Chemistry*, 85(3):1258–1263, February 2013.

[3] Shimon Weiss. Fluorescence Spectroscopy of Single Biomolecules. *Science*, 283(5408):1676–1683, March 1999.

[4] Elizabeth Rhoades, Eugene Gussakovsky, and Gilad Haran. Watching proteins fold one molecule at a time. *Proceedings of the National Academy of Sciences*, 100(6):3197–3202, March 2003.

[5] Harold Craighead. Future lab-on-a-chip technologies for interrogating individual molecules. *Nature*, 442(7101):387–393, July 2006.

[6] F. Ritort. Single-molecule experiments in biological physics: Methods and applications. *Journal of Physics: Condensed Matter*, 18(32):R531–R583, July 2006.

[7] Fredrik Persson, Irmeli Barkefors, and Johan Elf. Single molecule methods with applications in living cells. *Current Opinion in Biotechnology*, 24(4):737–744, August 2013.

[8] Michel Orrit, Taekjip Ha, and Vahid Sandoghdar. Single-molecule optical spectroscopy. *Chemical Society Reviews*, 43(4):973–976, January 2014.

[9] Sebastian van de Linde and Markus Sauer. How to switch a fluorophore: From undesired blinking to controlled photoswitching. *Chemical Society Reviews*, 43(4):1076–1087, January 2014.

[10] Zdeněk Farka, Matthias J. Mickert, Matěj Pastucha, Zuzana Mikušová, Petr Skládal, and Hans H. Gorris. Advances in Optical Single-Molecule Detection: En Route to Supersensitive Bioaffinity Assays. *Angewandte Chemie International Edition*, 59(27):10746–10773, 2020.

[11] W. E. Moerner and L. Kador. Optical detection and spectroscopy of single molecules in a solid. *Physical Review Letters*, 62(21):2535–2538, May 1989.

[12] W. E. (William E.) Moerner. Nobel Lecture: Single-molecule spectroscopy, imaging, and photocontrol: Foundations for super-resolution microscopy. *Reviews of Modern Physics*, 87(4):1183–1212, October 2015.

[13] M. Orrit and J. Bernard. Single pentacene molecules detected by fluorescence excitation in a p-terphenyl crystal. *Physical Review Letters*, 65(21):2716–2719, November 1990.

[14] Joseph R Lakowicz. *Principles of fluorescence spectroscopy*. Springer science & business media, 2013.

[15] Taekjip Ha, Alice Y. Ting, Joy Liang, W. Brett Caldwell, Ashok A. Deniz, Daniel S. Chemla, Peter G. Schultz, and Shimon Weiss. Single-molecule fluorescence spectroscopy of enzyme conformational dynamics and cleavage mechanism. *Proceedings of the National Academy of Sciences*, 96(3):893–898, February 1999.

[16] Shimon Weiss. Measuring conformational dynamics of biomolecules by single molecule fluorescence spectroscopy. *Nature Structural Biology*, 7(9):724–729, September 2000.

[17] W. E. Moerner and David P. Fromm. Methods of single-molecule fluorescence spectroscopy and microscopy. *Review of Scientific Instruments*, 74(8):3597–3619, August 2003.

[18] Manuel F Juette, Daniel S Terry, Michael R Wasserman, Zhou Zhou, Roger B Altman, Qinsi Zheng, and Scott C Blanchard. The bright future of single-molecule fluorescence imaging. *Current Opinion in Chemical Biology*, 20:103–111, June 2014.

[19] Lukas Novotny and Bert Hecht. *Principles of nano-optics*. Cambridge university press, 2012.

[20] Deep Punj, Mathieu Mivelle, Satish Babu Moparthi, Thomas S. van Zanten, Hervé Rigneault, Niek F. van Hulst, María F. García-Parajó, and Jérôme Wenger. A plasmonic 'antenna-in-box' platform for enhanced single-molecule analysis at micromolar concentrations. *Nature Nanotechnology*, 8(7):512–516, July 2013.

[21] Xuxing Lu, Gang Ye, Deep Punj, Ryan C. Chiechi, and Michel Orrit. Quantum Yield Limits for the Detection of Single-Molecule Fluorescence Enhancement by a Gold Nanorod. *ACS Photonics*, 7(9):2498–2505, September 2020.

[22] Weichun Zhang, Martín Caldarola, Xuxing Lu, and Michel Orrit. Plasmonic Enhancement of Two-Photon-Excited Luminescence of Single Quantum Dots by Individual Gold Nanorods. *ACS Photonics*, 5(7):2960–2968, July 2018.

[23] Oluwafemi S. Ojambati, Rohit Chikkaraddy, William M. Deacon, Junyang Huang, Demelza Wright, and Jeremy J. Baumberg. Efficient Generation of Two-Photon Excited Phosphorescence from Molecules in Plasmonic Nanocavities. *Nano Letters*, 20(6):4653–4658, June 2020.

[24] Gustav Mie. Beiträge zur Optik trüber Medien, speziell kolloidaler Metallösungen. *Annalen der Physik*, 330(3):377–445, 1908.

[25] R. H. Ritchie. Plasma Losses by Fast Electrons in Thin Films. *Physical Review*, 106(5):874–881, June 1957.

[26] Heinz Raether. Surface plasmons on smooth surfaces. In *Surface plasmons on smooth and rough surfaces and on gratings*, pages 4–39. Springer, 1988.

[27] Michael G Cottam and David R Tilley. *Introduction to surface and superlattice excitations*. CRC Press, 2019.

[28] Vladimir Moiseevich Agranovich. *Surface polaritons*. Elsevier, 2012.

[29] Jan Renger, Romain Quidant, Niek van Hulst, Stefano Palomba, and Lukas Novotny. Free-Space Excitation of Propagating Surface Plasmon Polaritons by Nonlinear Four-Wave Mixing. *Physical Review Letters*, 103(26):266802, December 2009.

[30] K. Lance Kelly, Eduardo Coronado, Lin Lin Zhao, and George C. Schatz. The Optical Properties of Metal Nanoparticles: The Influence of Size, Shape, and Dielectric Environment. *The Journal of Physical Chemistry B*, 107(3):668–677, January 2003.

[31] Matthew Rycenga, Claire M. Cobley, Jie Zeng, Weiyang Li, Christine H. Moran, Qiang Zhang, Dong Qin, and Younan Xia. Controlling the Synthesis and Assembly of Silver Nanostructures for Plasmonic Applications. *Chemical Reviews*, 111(6):3669–3712, June 2011.

[32] Uwe Kreibig and Michael Vollmer. *Optical properties of metal clusters*, volume 25. Springer Science & Business Media, 2013.

[33] Valerio Voliani. *Gold Nanoparticles*. De Gruyter, April 2020.

[34] Stephan Link and Mostafa A. El-Sayed. Size and Temperature Dependence of the Plasmon Absorption of Colloidal Gold Nanoparticles. *The Journal of Physical Chemistry B*, 103(21):4212–4217, May 1999.

[35] Huanjun Chen, Lei Shao, Qian Li, and Jianfang Wang. Gold nanorods and their plasmonic properties. *Chemical Society Reviews*, 42(7):2679–2724, 2013.

[36] Jorge Zuloaga, Emil Prodan, and Peter Nordlander. Quantum Plasmonics: Optical Properties and Tunability of Metallic Nanorods. *ACS Nano*, 4(9):5269–5276, September 2010.

[37] Jan Becker, Andreas Trügler, Arpad Jakab, Ulrich Hohenester, and Carsten Sönnichsen. The Optimal Aspect Ratio of Gold Nanorods for Plasmonic Bio-sensing. *Plasmonics*, 5(2):161–167, June 2010.

[38] Martin Dieter Baaske, Peter Sebastian Neu, and Michel Orrit. Label-Free Plasmonic Detection of Untethered Nanometer-Sized Brownian Particles. *ACS Nano*, 14(10):14212–14218, October 2020.

[39] Peter Zijlstra, Pedro M. R. Paulo, and Michel Orrit. Optical detection of single non-absorbing molecules using the surface plasmon resonance of a gold nanorod. *Nature Nanotechnology*, 7(6):379–382, June 2012.

[40] N. R. Jana, L. Gearheart, and C. J. Murphy. Seed-Mediated Growth Approach for Shape-Controlled Synthesis of Spheroidal and Rod-like Gold Nanoparticles Using a Surfactant Template. *Advanced Materials*, 13(18):1389–1393, 2001.

[41] J. Pérez-Juste, L. M. Liz-Marzán, S. Carnie, D. Y. C. Chan, and P. Mulvaney. Electric-Field-Directed Growth of Gold Nanorods in Aqueous Surfactant Solutions. *Advanced Functional Materials*, 14(6):571–579, 2004.

[42] Weihai Ni, Xiaoshan Kou, Zhi Yang, and Jianfang Wang. Tailoring Longitudinal Surface Plasmon Wavelengths, Scattering and Absorption Cross Sections of Gold Nanorods. *ACS Nano*, 2(4):677–686, April 2008.

[43] Hongwei Liao and Jason H. Hafner. Gold Nanorod Bioconjugates. *Chemistry of Materials*, 17(18):4636–4641, September 2005.

[44] Dakrong Pissuwan, Stella M. Valenzuela, and Michael B. Cortie. Prospects for Gold Nanorod Particles in Diagnostic and Therapeutic Applications. *Biotechnology and Genetic Engineering Reviews*, 25(1):93–112, January 2008.

[45] Xiaoge Hu and Xiaohu Gao. Multilayer coating of gold nanorods for combined stability and biocompatibility. *Physical Chemistry Chemical Physics*, 13(21):10028–10035, 2011.

[46] Peter Zijlstra, Pedro M. R. Paulo, Kuai Yu, Qing-Hua Xu, and Michel Orrit. Chemical Interface Damping in Single Gold Nanorods and Its Near Elimination by Tip-Specific Functionalization. *Angewandte Chemie*, 124(33):8477–8480, 2012.

[47] Pedro M. R. Paulo, Peter Zijlstra, Michel Orrit, Emilio Garcia-Fernandez, Tamara C. S. Pace, Ana S. Viana, and Sílvia M. B. Costa. Tip-Specific Functionalization of Gold Nanorods for Plasmonic Biosensing: Effect of Linker Chain Length. *Langmuir*, 33(26):6503–6510, July 2017.

[48] E. Prodan, C. Radloff, N. J. Halas, and P. Nordlander. A Hybridization Model for the Plasmon Response of Complex Nanostructures. *Science*, 302(5644):419–422, October 2003.

[49] T. J. Davis, D. E. Gómez, and K. C. Vernon. Simple Model for the Hybridization of Surface Plasmon Resonances in Metallic Nanoparticles. *Nano Letters*, 10(7):2618–2625, July 2010.

[50] Boris Luk'yanchuk, Nikolay I. Zheludev, Stefan A. Maier, Naomi J. Halas, Peter Nordlander, Harald Giessen, and Chong Tow Chong. The Fano resonance in plasmonic nanostructures and metamaterials. *Nature Materials*, 9(9):707–715, September 2010.

[51] Liane S. Slaughter, Yanpeng Wu, Britain A. Willingham, Peter Nordlander, and Stephan Link. Effects of Symmetry Breaking and Conductive Contact on the Plasmon Coupling in Gold Nanorod Dimers. *ACS Nano*, 4(8):4657–4666, August 2010.

[52] Jatish Kumar, Xingzhan Wei, Steven Barrow, Alison M. Funston, K. George Thomas, and Paul Mulvaney. Surface plasmon coupling in end-to-end linked gold nanorod dimers and trimers. *Physical Chemistry Chemical Physics*, 15(12):4258–4264, February 2013.

[53] Xuxing Lu, Jian Wu, Qiannan Zhu, Junwei Zhao, Qiangbin Wang, Li Zhan, and Weihai Ni. Circular dichroism from single plasmonic nanostructures with extrinsic chirality. *Nanoscale*, 6(23):14244–14253, 2014.

[54] Maria Göppert-Mayer. über Elementarakte mit zwei Quantensprüngen. *Annalen der Physik*, 401(3):273–294, 1931.

[55] Patrick Theer, Mazahir T. Hasan, and Winfried Denk. Two-photon imaging to a depth of 1000 Mm in living brains by use of a Ti:Al_2O_3 regenerative amplifier. *Optics Letters*, 28(12):1022–1024, June 2003.

[56] Fritjof Helmchen and Winfried Denk. Deep tissue two-photon microscopy. *Nature Methods*, 2(12):932–940, December 2005.

[57] W. Denk, J. H. Strickler, and W. W. Webb. Two-photon laser scanning fluorescence microscopy. *Science*, 248(4951):73–76, April 1990.

[58] C. J. R SHEPPARD and M. GU. Image formation in two-photon fluorescence microscopy. *Image formation in two-photon fluorescence microscopy*, 86(3):104–106, 1990.

[59] Min Gu and C. J. R. Sheppard. Comparison of three-dimensional imaging properties between two-photon and single-photon fluorescence microscopy. *Journal of Microscopy*, 177(2):128–137, 1995.

[60] William A. Mohler, Jeffrey S. Simske, Ellen M. Williams-Masson, Jeffrey D. Hardin, and John G. White. Dynamics and ultrastructure of developmental cell fusions in the Caenorhabditis elegans hypodermis. *Current Biology*, 8(19):1087–1091, September 1998.

[61] Jayne M. Squirrell, David L. Wokosin, John G. White, and Barry D. Bavister. Long-term two-photon fluorescence imaging of mammalian embryos without compromising viability. *Nature Biotechnology*, 17(8):763–767, August 1999.

[62] P. A. Franken, A. E. Hill, C. W. Peters, and G. Weinreich. Generation of Optical Harmonics. *Physical Review Letters*, 7(4):118–119, August 1961.

[63] W. Kaiser and C. G. B. Garrett. Two-Photon Excitation in Ca${\mathrm{F}}_{2}$: ${\mathrm{Eu}}^{2+}$. *Physical Review Letters*, 7(6):229–231, September 1961.

[64] Marius A. Albota, Chris Xu, and Watt W. Webb. Two-photon fluorescence excitation cross sections of biomolecular probes from 690 to 960 nm. *Applied Optics*, 37(31):7352–7356, November 1998.

[65] Amit Nag and Debabrata Goswami. Solvent effect on two-photon absorption and fluorescence of rhodamine dyes. *Journal of Photochemistry and Photobiology A: Chemistry*, 206(2):188–197, August 2009.

[66] Chris Xu and Watt W. Webb. Measurement of two-photon excitation cross sections of molecular fluorophores with data from 690 to 1050 nm. *JOSA B*, 13(3):481–491, March 1996.

[67] Saumyakanti Khatua, Pedro M. R. Paulo, Haifeng Yuan, Ankur Gupta, Peter Zijlstra, and Michel Orrit. Resonant Plasmonic Enhancement of Single-Molecule Fluorescence by Individual Gold Nanorods. *ACS Nano*, 8(5):4440–4449, May 2014.